Available online at www.sciencedirect.com
SCIENCE DIRECT®
Biochimica et Biophysica Acta 1661 (2004) 18–25
BIOCHIMICA ET BIOPHYSICA ACTA
BBA
www.bba-direct.com

Diffusion and dynamics of penetratin in different membrane mimicking media

August Andersson, Jonas Almqvist, Franz Hagn, Lena Mäler*

Department of Biochemistry and Biophysics, Arrhenius Laboratory, Stockholm University, 10691 Stockholm, Sweden

Received 6 August 2003; received in revised form 14 November 2003; accepted 20 November 2003

Abstract

The interaction between the cell-penetrating peptide (CPP) penetratin and different membrane mimetic environments has been investigated by two different NMR methods: ^{15}N spin relaxation and translational diffusion. Diffusion coefficients were measured for penetratin in neutral and in negatively charged bicelles of different size, in sodium dodecyl sulfate micelles (SDS), and in aqueous solution. The diffusion coefficients were used to estimate the amount of free and bicelle/micelle-bound penetratin and the results revealed that penetratin binds almost fully to all studied membrane mimetics. ^{15}N relaxation data for three sites in penetratin were interpreted with the model-free approach to obtain overall and local dynamics. Overall correlation times for penetratin were in agreement with findings for other peptides of similar size in the same solvents. Large differences in order parameters were observed for penetratin in the different membrane mimetics. Negatively charged surfaces were seen to restrict motional flexibility, while a more neutral membrane mimetic did not. This indicates that although the peptide binds to both bicelles and SDS micelles, the interaction between penetratin and the various membrane mimetics is different.

Keywords: Penetratin; Bicelle; NMR; ^{15}N relaxation; Dynamics; PFG; Diffusion

1. Introduction

Cell-penetrating peptides (CPP) have the ability to translocate cell membranes with high efficiency. If they are covalently linked to a larger cargo, such as polypeptides or oligonucleotides, they still retain their translocating properties [1]. One such peptide is penetratin, or pAnt, which has the sequence RQIKIWFQNRRMKWKK derived from the third helix of the Antennapedia homeodomain of the *Drosophila* transcription factor. In order to understand the details in the translocation process, extensive structural studies of penetratin in the presence of membrane mimetic solvents have been performed [2–7]. The structure, however, does not seem to play a crucial role for the translocation mechanism [1,8]. Other factors, such as motional flexibility, could be important in defining the interaction between the membrane and the peptide.

Detergent micelles have long been used as membrane mimicking media in NMR investigations, but lately two-component micelles, bicelles, have been used as an experimental membrane model [9,10]. These bicelles are generally composed of a mixture of phospholipids and detergents. It has been shown that peptide structure can be influenced by the small size and shape of detergent micelles [11], which in turn might influence the conclusions on membrane interactions. It has also been shown that small detergent micelles can impose restrictions in local motion, depending on the properties of the peptide [12]. The bicelles are believed to provide a better membrane mimetic, since they contain a well-defined phospholipid bilayer region. The size and shape of a bicelle are defined by the ratio between the amount of lipids and detergents, the q-value. Small, isotropically tumbling bicelles have been characterized by several techniques,

Abbreviations: CPP, cell-penetrating peptide; SDS, sodium dodecyl sulfate; DHPC, 1,2-dihexanoyl-*sn*-glycero-3-phosphatidylcholine; DMPC, 1,2-dimyristoyl-*sn*-glycero-3-phosphatidylcholine; DMPG, 1,2-dimyristoyl-*sn*-glycero-3-phospho-1-glycerol; TOCSY, total correlation spectroscopy; HSQC, heteronuclear single quantum coherence; TROSY, transverse relaxation-optimized spectroscopy; PFG, pulsed field gradient; CD, circular dichroism

* Corresponding author. Tel.: +46-8-162448; fax: +46-8-155597.
E-mail address: lena@dbb.su.se (L. Mäler).

0005-2736/$ - see front matter © 2003 Elsevier B.V. All rights reserved.
doi:10.1016/j.bbamem.2003.11.014

and they have been found to be disk-shaped objects, with a phospholipid bilayer region surrounded by a detergent rim [13,14]. These aggregates have been used successfully in high resolution NMR structure and dynamics investigations of peptide-membrane interactions [5,9,11,12,15].

In this study the interactions between the cell-penetrating peptide penetratin and different bicelles and sodium dodecyl sulfate (SDS) micelles have been investigated by two NMR-approaches, ^{15}N relaxation and translational diffusion. Both of these methods provide information about the size of the peptide-bicelle/micelle complex, but are complementary in other senses. By comparing translational diffusion coefficients from different chemical species, such as the phospholipids, detergents and peptide, it is possible to calculate the population of these species in different states, such as bound to a bicelle or micelle, or free in solution. Relaxation, on the other hand, can give insights on overall reorientation of the peptide-bicelle/micelle complex, as well as on how different interactions affect the local motion of the peptide. These two methods can together provide an estimate of the amount of bicelle/micelle-bound peptide, and on how the local dynamics are influenced by different membrane mimetic media.

2. Experimental

2.1. Materials

Commercial penetratin was obtained from Neosystem Labs and used as received. Three sites in penetratin were labeled with ^{15}N, the backbone nitrogen atom in residues Ile3, Ile5 and Phe7. Phospholipids, dimyristoyl-*sn*-glycero-phosphatidylcholine (DMPC), dimyristoyl-*sn*-glycero-phosphatidyl-glycerol (DMPG) and dihexanoyl-*sn*-glycero-phosphatidylcholine (DHPC) were obtained from Larodan or Avanti Polar lipids. All samples were prepared with 3 mM penetratin in 50 mM KCl solution, and the pH was adjusted to 5.5 ± 0.1. The total concentration of lipids and detergents was 300 mM in both the bicelle and the SDS samples. The size of the bicelle is roughly determined by the q-value, which is the molar amount of long-chained lipids divided by the molar amount of detergent. Three bicelle samples were made, two acidic with $q = 0.15$ and $q = 0.5$, and one neutral with $q = 0.5$. Bicelle samples were prepared by adding a stock solution of DHPC to a mixture of long-chained lipids and peptide as described previously [9]. The acidic bicelle samples were produced by replacing 10% of the DMPC by DMPG [16]. The SDS sample was prepared by adding peptide to a SDS solution. All samples contained $\sim$ 10% $^{2}H_2O$ for field/frequency locking.

2.2. NMR spectroscopy

The NMR spectra were obtained using Varian Inova spectrometers, operating at 400, 600 and 800 MHz ^{1}H-frequency, all equipped with a triple-resonance probe-head, and on a Bruker Avance spectrometer operating at 400-MHz ^{1}H-frequency using a doubleresonance probe-head. All experiments were carried out at 37 °C and the temperature was calibrated using a thermocouple, which was inserted into a regular NMR tube containing H_2O. TOCSY [17] spectra were recorded at 600 MHz in pure absorption mode using the States method [18] with 2048 complex data points in the directly detected dimension and 512 in the indirectly detected dimension. Water suppression was performed by low power presaturation on the water frequency. 2D data processing included zero filling to 4096 points in both dimensions. Sensitivity-enhanced $^{1}H-^{15}N$ HSQC and $^{1}H-^{15}N$ TROSY [19] spectra were recorded at 800 MHz, with 1024 complex data points in the directly detected dimension and 256 in the indirect dimension.

The translational diffusion measurements were carried out at 600 MHz using modified versions of the Stejskal–Tanner spin-echo experiment [20,21]. Data were recorded by using a minimum of 32 scans, and by using 30 linearly spaced values of increasing gradient strength. Problems with nonlinear gradients were accounted for according to Damberg et al. [22]. The translational diffusion coefficients were obtained by fitting peak integrals to the modified Stejskal–Tanner equation. To account for inaccuracies in determining the translational diffusion coefficients due to fast chemical exchange between species of unequal relaxation, the T_1-delay time in the pulse sequence was incremented. The gradient strength (g) was chosen from increasing T_1-delays (d) as

$$g^2 d = \text{constant} \quad (1)$$

A linear equation was fitted to the linear region of the resulting plot, and the translational diffusion coefficients were obtained by extrapolating to $d = 0$. The diffusion of water was measured in all samples as a marker for viscosity differences.

Inverse-detected relaxation measurements [23] were recorded as 1D spectra. T_1, T_2 and steady-state NOE factors were recorded at a minimum of two magnetic field strengths. All spectra were recorded with at least 512 scans. T_1 and T_2 relaxation times were calculated from exponential fits with a minimum of 12 relaxation delays. NOE factors were calculated by comparing signal amplitudes obtained with and without proton decoupling. Errors were estimated from duplicate spectra. A conservative error estimate was, however, used for the final fitting procedure and no error was set to be lower than 5%.

2.3. Analysis of translational diffusion data

The translational diffusion coefficients were used to estimate binding populations of penetratin to the membrane mimicking aggregates [24,25]. By using the diffusion rates of the long-chained phospholipids as indicators for bicelle diffusion and by measuring the diffusion of the free peptide

and DHPC, the populations of free and bicelle-bound peptide and DHPC can be estimated from

$$x \cdot D_{\text{bound}} + (1-x) \cdot D_{\text{free}} \cdot \left(\frac{D_{\text{H}_2\text{O,complex}}}{D_{\text{H}_2\text{O,free}}} \right) = D_{\text{complex}} \quad (2)$$

where x is the amount of molecules bound to the bicelle. D_{bound} is the diffusion of the bicelle as determined from the DMPC/DMPG diffusion coefficients, D_{free} is the diffusion coefficient for the free molecule, i.e. penetratin or DHPC, and D_{complex} is the diffusion coefficient for penetratin or DHPC in the presence of bicelles. The diffusion coefficients for water, D_{H2O}, are introduced to account for differences in viscosity in the different solutions. An analogous approach was used for determining the amount of bound and free penetratin in SDS micelles. The methyl resonances in DMPC and DHPC were chosen to monitor the diffusion of the aggregate and the aromatic/amide region of the penetratin spectrum was used to monitor penetratin diffusion.

2.4. Analysis of relaxation data

Relaxation data were analyzed by using the model-free approach for spectral densities [26–28] and the fitting was done with the Modelfree 4.01 software [29,30]. For selecting the appropriate model for the spectral density function, the scheme by Mandel et al. [29] was used. A simple model with only an overall correlation time, τ_m, and a generalized order parameter, S^2, was first tested and additional parameters were then added until a good fit was obtained, as determined by a statistical F-test. No global overall correlation times for the entire peptide were calculated, due to the unknown anisotropic rotation of the different complexes. Therefore local overall correlation times were calculated for each site. The chemical shift anisotropy, which was assumed to be axially symmetric, was set to -163 ppm [31], and a $^1H-^{15}N$ inter-nuclear distance of 1.04 Å was used [32].

3. Results

3.1. Assignment of Ile3, Ile5 and Phe7 amide resonances

A TOCSY spectrum with a mixing time of 60 ms was recorded for the ^{15}N-labeled penetratin in aqueous solution and in $q=0.15$ acidic bicelle solution. Three peaks in the spectrum contained clear doublets from the $^1H-^{15}N$ J-coupling. The Phe7 doublet was easily identified from couplings to H^{β} side-chain protons. The assignments for the isoleucine residues were guided by previous assignment for penetratin in $q=0.5$ bicelles and the great similarities between spectra for penetratin in acidic $q=0.5$ and $q=0.15$ bicelles. A $^1H-^{15}N$ TROSY spectrum was recorded for the acidic $q=0.5$ sample to investigate the possibility that larger aggregates with signals not visible in conventional HSQC exist. No such existence was found as the two spectra showed essentially similar features (Fig. 1).

3.2. Translational diffusion

Translational diffusion measurements were conducted for penetratin in aqueous solution, in SDS-micelles, in neutral and acidic $q=0.5$ bicelles, and for penetratin in $q=0.15$ acidic bicelles. In order to properly account for the possibility that penetratin exists in both a bound and a free form, relaxation effects during the T_1-delay (d in Eq. (1)) in the experiment must be accounted for. Therefore, we measured the diffusion coefficients from a series of experiments with increasing T_1-delay values and extrapolated the diffusion coefficients to zero delay time (Fig. 2). Diffusion

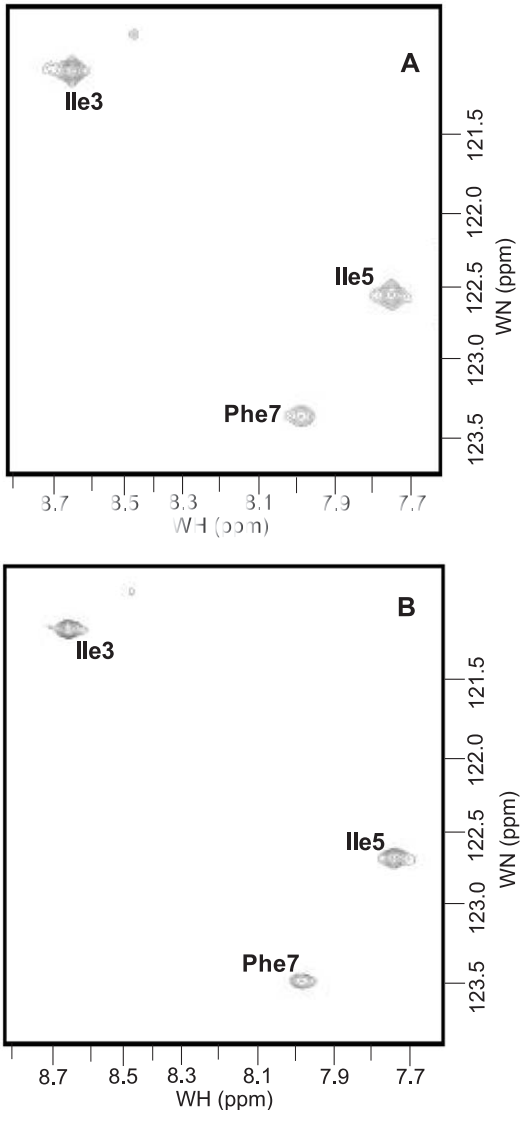

Fig. 1. Contour plots of two-dimensional $^1H-^{15}N$-HSQC (A), and $^1H-^{15}N$ TROSY (B) spectra for penetratin in $q=0.5$ acidic bicelles ([DMPG]/[DMPC]=0.1) recorded at a ^1H frequency of 800 MHz and at 37 °C.

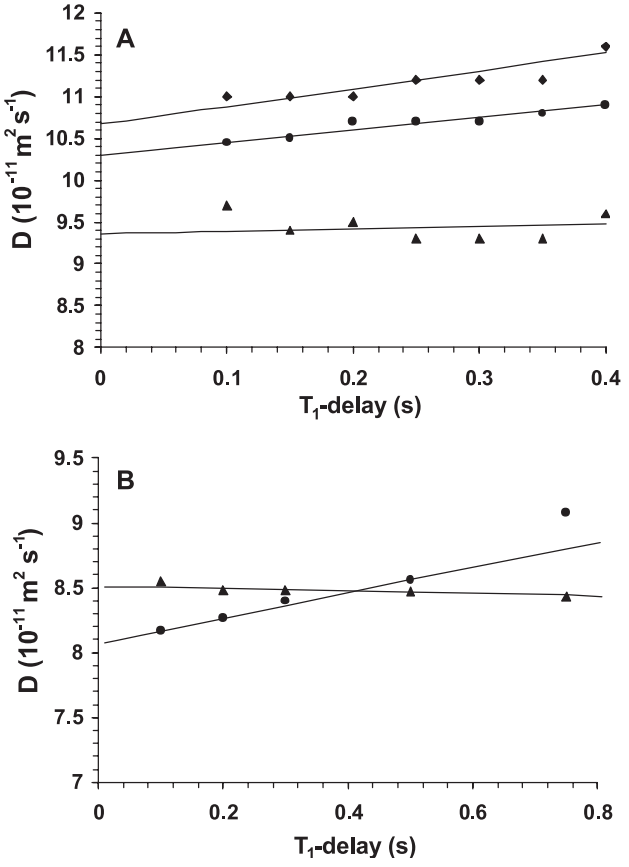

Fig. 2. Dependence of the translational diffusion coefficient on the T_1-delay time for (A) penetratin in $q=0.15$ acidic bicelles at 37 °C, and (B) penetratin in SDS-micelles at 37 °C. In (A), circles show diffusion coefficients for penetratin, diamonds show diffusion coefficients for DHPC, and triangles show diffusion coefficients for DMPC. In (B), circles show diffusion coefficients for penetratin, and triangles show diffusion coefficients for SDS. The solid lines show the mean T_1 dependence of the diffusion coefficient in the linear region.

coefficients obtained in this way for penetratin, SDS, the phospholipids, and for H_2O are collected in Table 1. The diffusion of penetratin in aqueous solution is somewhat slower than what may be expected for a peptide of this size [33], which may be indicative of peptide aggregation. In order to investigate this, diffusion coefficients were therefore measured at three peptide concentrations (3, 7.5 and 10 mM). The diffusion coefficients for penetratin were indeed found to be concentration-dependent, which shows that penetratin aggregates somewhat (Fig. 3). This makes calculations of the amount of bound and free peptide difficult. However, one should note that since the diffusion rate is faster at lower peptide concentrations, the estimated fraction of bound peptide in the bicelle/micelle samples will be underestimated, and thus a minimum fraction of bound peptide can be calculated using Eq. (2). Using this approach, it can clearly be seen that penetratin interacts with all membrane mimetics. The results show that at least 95% of penetratin is bound to all bicelles, and that penetratin also interacts strongly with SDS micelles. From the results obtained for penetratin in the different bicelle solutions, one can also note that the DMPC lipids diffuse slower than DHPC, indicating that the DHPC molecules exist not only in a bicelle-bound form (Table 1). This has previously been investigated and it has been shown that an amount of around 10 mM DHPC is free in solution under a wide range of conditions [25,34]. The dependence of the diffusion coefficient on the T_1-delay (d in Eq. (1)) contains information about the distribution between small and large aggregates in solution. For a distribution of large (e.g., bicelles) and small (e.g., phospholipids) objects in solution, one would expect an increase in diffusion coefficient with increasing T_1 delay, provided that the smaller objects have slower T_1 relaxation than the large objects. In Fig. 2A, the dependence on the T_1 delay is shown for penetratin, DMPC/DMPG, and DHPC in $q=0.15$ acidic bicelles. The apparent diffusion coefficients for penetratin and DHPC are clearly seen to increase slightly with increasing T_1 delay, while the diffusion constant for DMPC remains constant. This indicates that all of the long-chained DMPC/DMPG phospholipids are in the bicelle-bound form, while a small fraction of the DHPC and penetratin molecules exist not only in the

Table 1
Translational diffusion coefficients for penetratin and the bicelle/micelle components in the different membrane mimetics

D_{obs} ($\times 10^{-11}$ m^2 s^{-1})					
Solvent	Penetratin	DHPC	DMPC	SDS	H_2O
H_2O (3 mM peptide)	28 ± 0.1				329 ± 2
H_2O (7.5 mM peptide)	26.3 ± 0.1				316 ± 2
H_2O (10 mM peptide)	26.1 ± 0.1				317 ± 2
SDS	8.1 ± 0.1			8.5 ± 0.1	300 ± 3
Acidic bicelles, $q=0.15$	10.3 ± 0.1	10.7 ± 0.1	9.4 ± 0.1		280 ± 2
Acidic bicelles, $q=0.5$	2.4 ± 0.1	4.3 ± 0.1	1.9 ± 0.1		280 ± 4
Neutral bicelles, $q=0.5$	2.7 ± 0.1	4.5 ± 0.1	2.5 ± 0.1		270 ± 4

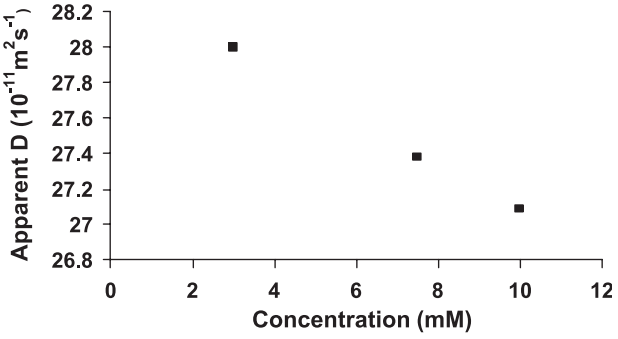

Fig. 3. The translational diffusion coefficient for penetratin plotted against concentration. The differences in viscosity are taken into account by normalizing against the diffusion coefficients for H_2O. The viscosity for the 3 mM sample is normalized to 1.

bicelle-bound form, but also, either as monomers in solution or in smaller micellar aggregates. This agrees with previous results indicating that around 10 mM DHPC, corresponding to less than 5% of the total amount of DHPC in the $q=0.15$ bicelle sample, exists as monomers in solution. It seems realistic that the similar T_1 delay dependence observed for penetratin corresponds to a comparable amount of free peptide in solution, leading to an estimate of around 95% of penetratin being bound to the bicelles. The trends in the other two bicellar solvents, $q=0.5$ acidic and neutral bicelles, are similar (data not shown) and again in agreement with a large amount of penetratin being in the bicelle-bound state.

From the diffusion data for penetratin in SDS, it is seen that the peptide is in principle fully bound to the SDS micelles, but the finding that the SDS molecules, on average, diffuse slightly faster than penetratin is intriguing (Table 1). One explanation for this is that the SDS micelle-to-penetratin ratio, assuming 60 SDS molecules/micelle [35], is roughly 5:3. This means that it is possible that all penetratin molecules interact with SDS micelles, leaving a certain amount of SDS molecules that, on average, do not interact with penetratin, and thus exist in either monomeric form, or in micelles without penetratin. It is difficult to determine which of these explanations, or indeed a combination of the two, is correct. Nevertheless, the T_1 dependence suggests that virtually all of the SDS molecules are micelle-bound, while a certain fraction of penetratin is free in solution Fig. 2B. The faster SDS diffusion can then be explained by the higher concentration of micelles as compared to penetratin and that the micelles become, on average, slightly larger when penetratin is bound. This size difference is not large enough to have a significant impact on the T_1 delay dependence.

3.3. Analysis of relaxation data

In order to characterize the dynamics of penetratin, R_1, R_2 and NOE relaxation data were measured at several fields for three ^{15}N-labeled backbone amide sites, Ile3, Ile5 and Phe7. Measurements were carried out in aqueous solution, in acidic $q=0.15$ and $q=0.5$ bicelles, and in SDS (Table 2). The multiple-field relaxation data were analyzed within the framework of the model-free approach. The quality of the model-free fit can be seen in Fig. 4 and the results from the fitting procedure are summarized in Table 3. To account for possible anisotropic overall reorientation, local overall correlation times (τ_{loc}) were calculated individually for the three different sites. The data for penetratin in H_2O, $q=0.5$ bicelles and SDS all converged with the same model, which contained an overall correlation time, a generalized order parameter (S^2) and a correlation time for the local motion (τ_e). In order to fit the data for penetratin in $q=0.15$ bicelles, an additional order parameter, describing a faster local motion (S^2_f), was needed [36]. No fast exchange terms were needed in any of the fits as the field-dependence of the R_2 rates could adequately be described by CSA relaxation (Fig. 4).

Site variations in the overall correlation times for penetratin are observed in all membrane mimetic media, as well as in H_2O, although not to a large extent. This variation may be an indication of anisotropic rotational tumbling motion. However, it must be pointed out that the overall correlation times are associated with rather high errors, making conclusions on anisotropy difficult. The overall correlation times for penetratin in aqueous solution (average 2 ns) are slightly longer than what may be expected for a monomeric peptide of this size [37]. This is in agreement with the results obtained from the diffusion data, indicating that penetratin undergoes some aggregation. The apparent size of the penetratin–SDS micelle complex, as judged by the overall correlation time (average 7.5 ns), is comparable to the apparent size of penetratin in $q=0.15$ bicelles (average 7.4 ns). The diffusion is similar for the two media, supporting the observation that they are similar in size. The overall correlation time for penetratin is qualitatively in agreement

Table 2
Relaxation data for the ^{1}H–^{15}N backbone spin-pairs in residues Ile3, Ile5 and Phe7 in penetratin in $q=0.15$ acidic bicelles, $q=0.5$ acidic bicelles, SDS, and aqueous solution

Solvent	B_0 (T)	Site	R_1 (s^{-1})	R_2 (s^{-1})	NOE
H_2O	9.39	Ile3	1.08 ± 0.05	1.26 ± 0.05	− 1.2 ± 0.1
		Ile5	1.38 ± 0.06	1.85 ± 0.09	− 0.7 ± 0.1
		Phe7	1.45 ± 0.07	1.47 ± 0.07	− 0.67 ± 0.1
	18.8	Ile3	0.95 ± 0.02	1.76 ± 0.09	− 0.8 ± 0.1
		Ile5	1.24 ± 0.02	1.95 ± 0.09	− 0.3 ± 0.1
		Phe7	1.32 ± 0.02	2.20 ± 0.09	− 0.1 ± 0.1
Acidic bicelles $q=0.15$	9.39	Ile3	1.87 ± 0.09	4.4 ± 0.2	− 0.1 ± 0.1
		Ile5	2.1 ± 0.1	5.7 ± 0.3	0.2 ± 0.1
		Phe7	2.2 ± 0.1	5.9 ± 0.3	0.3 ± 0.1
	14.09	Ile3	1.43 ± 0.07	4.5 ± 0.2	0.1 ± 0.1
		Ile5	1.56 ± 0.08	6.9 ± 0.3	0.4 ± 0.1
		Phe7	1.63 ± 0.08	7.0 ± 0.4	0.3 ± 0.1
	18.8	Ile3	1.28 ± 0.07	5.5 ± 0.3	0.4 ± 0.1
		Ile5	1.30 ± 0.07	9.0 ± 0.4	0.5 ± 0.1
		Phe7	1.34 ± 0.07	8.1 ± 0.4	0.5 ± 0.1
Acidic bicelles $q=0.5$	9.39	Ile3	1.7 ± 0.1		
		Ile5	1.6 ± 0.1		
		Phe7	1.8 ± 0.1		
	14.09	Ile3	1.17 ± 0.06	18.4 ± 0.9	
		Ile5	1.03 ± 0.05	19.9 ± 1.0	
		Phe7	1.03 ± 0.05	19.8 ± 1.0	
	18.8	Ile3	1.00 ± 0.05	20 ± 1	0.5 ± 0.1
		Ile5	0.84 ± 0.04	24.9 ± 1.3	0.6 ± 0.1
		Phe7	0.85 ± 0.04	22.6 ± 1.1	0.65 ± 0.10
SDS	9.39	Ile3	2.18 ± 0.04	6.56 ± 0.04	0.5 ± 0.1
		Ile5	2.29 ± 0.01	6.59 ± 0.05	0.5 ± 0.1
		Phe7	2.69 ± 0.03	6.9 ± 0.6	0.5 ± 0.1
	14.09	Ile3	1.65 ± 0.01	7.11 ± 0.05	0.6 ± 0.1
		Ile5	1.68 ± 0.03	7.63 ± 0.04	0.5 ± 0.1
		Phe7	1.80 ± 0.01	7.91 ± 0.02	0.7 ± 0.1
	18.8	Ile3	1.29 ± 0.01	8.5 ± 0.1	
		Ile5	1.32 ± 0.02	9.04 ± 0.09	
		Phe7	1.38 ± 0.01	9.49 ± 0.06	

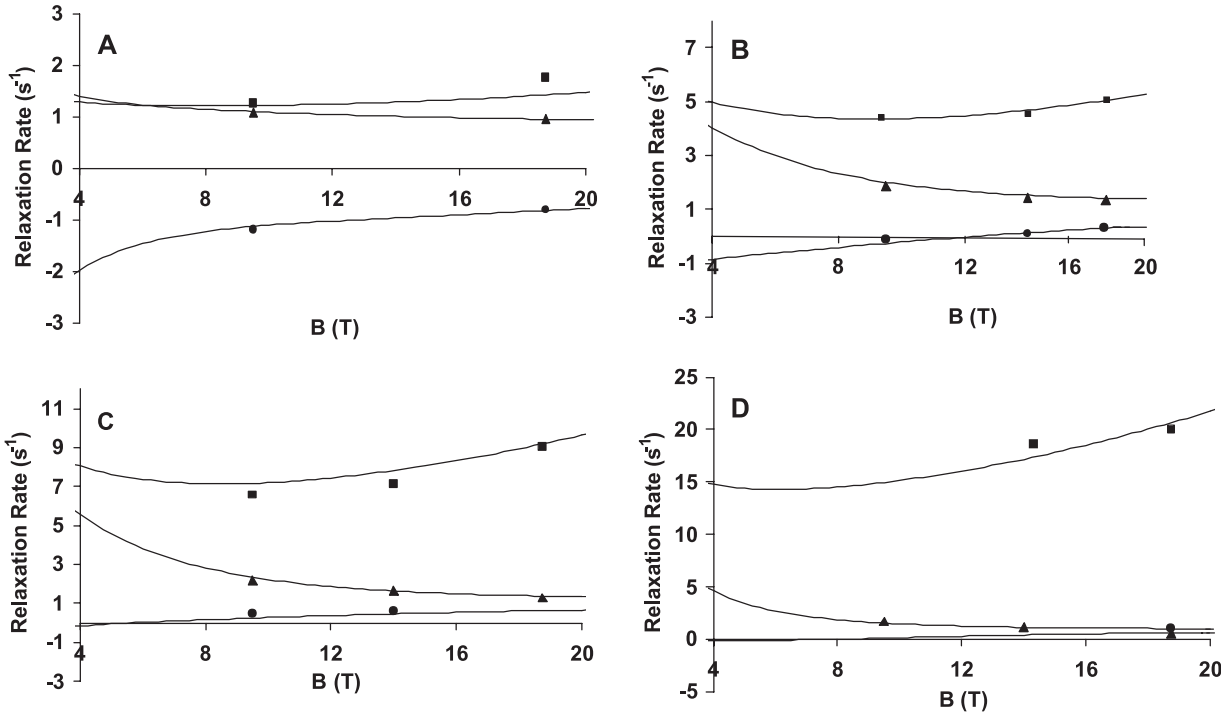

Fig. 4. Relaxation data for Ile3 in penetratin in aqueous solution (A), $q=0.15$ bicelles (B), SDS (C), and in $q=0.5$ acidic bicelles (D). Experimentally determined R_1 values are depicted as triangles, R_2 values are shown as squares and NOE-factors are shown as circles. The solid lines indicate theoretically calculated values for the relaxation rates, obtained from the model-free parameters.

with what has previously been found for the peptide hormone motilin in SDS micelles [37]. The overall rotational correlation times for penetratin in acidic $q=0.5$ bicelles are, as expected, much longer than what is observed in the smaller SDS micelles and $q=0.15$ bicelles. Again, this result is supported by the differences observed in the diffusion data. The correlation times are longer than what has previously been seen for the small peptide hormone motilin interacting with bicelles of equal size [12]. This is, however, strongly dependent on the relative angle of the spin-vector compared to the main axis of rotational anisotropy. Nevertheless, a qualitative agreement with the previous results is seen.

The generalized order parameters, S^2, measured for the three sites in penetratin generally follow a simple trend in all solvents, indicating that the peptide is more flexible at the N-terminus, and that the rigidity increases sequentially. This is physically reasonable since one expects the termini to be less structured. The generalized order parameters observed in H_2O are, as expected, consistent with a highly flexible peptide. Thus, even though a certain degree of aggregation occurs, as suggested by the diffusion data and overall correlation times, the dynamics for the measured sites clearly indicated a high degree of flexibility as expected for a small peptide in solution. The highest order parameters for penetratin are observed in the $q=0.5$ bicelles (0.66–0.82), indicative of restricted local motion. The relatively high order parameters for penetratin in SDS micelles (0.65–0.77) indicate that the local motion is restricted also in this solvent, however, not as much as in the $q=0.5$ bicelles. The major difference is that there seems to be a larger flexible region at the N-terminus of the peptide, as evidenced by the lower order parameter for Ile5 in SDS. The lowest order parameters are observed in the slightly acidic $q=0.15$ bicelles (0.39–0.60). However, a direct comparison with the other data is complicated by the need for an additional order parameter (S^2_f) to explain the relaxation data. The presence of S^2_f reveals

Table 3
Model-free dynamic parameters for the $^1H-^{15}N$ backbone spin-pairs in residues Ile3, Ile5 and Phe7 in penetratin in H_2O, SDS, $q=0.15$ acidic bicelles, and in $q=0.5$ acidic bicelles

	Site	τ_{loc} (ns)	S^2	S^2_f	τ_e (ns)
H_2O	Ile3	2.3 ± 0.1	0.23 ± 0.01		0.12 ± 0.01
	Ile5	2.0 ± 0.1	0.38 ± 0.01		0.13 ± 0.01
	Phe7	1.8 ± 0.1	0.44 ± 0.02		0.11 ± 0.01
$q=0.15$	Ile3	6.9 ± 0.6	0.39 ± 0.04	0.84 ± 0.02	0.9 ± 0.1
	Ile5	8.0 ± 0.7	0.55 ± 0.05	0.93 ± 0.03	1.0 ± 0.2
	Phe7	7.3 ± 0.6	0.60 ± 0.06	0.95 ± 0.03	1.0 ± 0.2
$q=0.5$	Ile3	19.3 ± 1.6	0.66 ± 0.05		1.2 ± 0.2
	Ile5	19.4 ± 1.2	0.79 ± 0.04		1.4 ± 0.3
	Phe7	17.4 ± 1.0	0.82 ± 0.03		1.9 ± 0.6
SDS	Ile3	8.0 ± 0.6	0.65 ± 0.05		1.1 ± 0.2
	Ile5	7.7 ± 0.6	0.67 ± 0.06		1.3 ± 0.2
	Phe7	6.9 ± 0.6	0.77 ± 0.08		1.4 ± 0.4

a significant difference in dynamics between penetratin in $q = 0.15$ bicelles and in the other media.

4. Discussion

The translational diffusion data surprisingly indicate that penetratin interacts with all membrane mimicking media used in this study. Magzoub et al. [4] have previously shown that penetratin does not interact with neutral phospholipid vesicles. On the other hand, they showed that by introducing as little as 2 mol% negative charges, 75% of the peptide becomes bound to the vesicles. A direct comparison with the present results is, however, difficult since the measurements were performed at very different overall concentrations as well as different lipid/peptide ratios. Nevertheless, the observation that penetratin does interact with neutral bicelles indicates that the bicelles do not have the same properties as the vesicles. The bicelles contain a highly soluble detergent rim, which could very well be responsible for the penetratin–bicelle interaction. On the other hand, differences in circular dichroism (CD) spectra of penetratin in neutral bicelles and in DHPC have previously been observed [5]. These observations together with the present results suggest that it is likely that penetratin interacts very differently with the neutral and charged bicelles. Around 95% of the total amount of penetratin seems to be bound to the negatively charged bicelles, which is in agreement with results in negatively charged vesicles [4].

When comparing the diffusion of neutral and acidic $q = 0.5$ bicelles, interesting observations are made. The presence of penetratin alters the apparent size of the acidic and neutral bicelles in different ways. The diffusion coefficients show that the acidic bicelles are larger than the neutral bicelles when penetratin is present. Comparing to earlier results obtained for bicelles without peptides [25] and accounting for differences in viscosity, the diffusion coefficient for both acidic and neutral bicelles in the absence of peptide is found to be $2.6 \times 10-11$ m^2/s. Comparing this to the data in Table 1 shows that the acidic bicelles diffuse slower in the presence of penetratin. Thus, one might argue that penetratin makes the acidic bicelles apparently larger, whereas the apparent size of the neutral bicelles remains the same. This further supports the conclusion that penetratin interacts differently with the neutral and charged bicelles. The change in diffusion coefficient may stem from changes in size distributions of the bicelles upon peptide binding, but also from changes in bicelle morphology.

The diffusion results, indicating that a large amount of peptide is bound to all mimetics, are important when discussing the relaxation data, since the contribution of a free form to the observed dynamics can safely be neglected. The dynamics of penetratin in $q = 0.5$ acidic bicelles shows that the peptide has a flexible N-terminus (Ile3) with a more rigid core (Ile5 and Phe7). This is in good agreement with the structure of penetratin in the same medium, where the N-terminus is unstructured and an α-helix is present for residues Lys4 through Met12 [5].

Turning to the dynamics results for penetratin, it is observed that local dynamics are highly dependent on bicelle size. The need for a second generalized order parameter for penetratin in the presence of small ($q = 0.15$) bicelles is an indication of complex local dynamics with two time-scales. The low overall order parameters may be due to two factors. The smaller bicelle has a higher degree of curvature as compared to the $q = 0.5$ bicelles, and, perhaps more important, has less charge per bicelle aggregate. Since penetratin has similar local dynamics in SDS micelles, which are small and spherical but with a high charge density, as in $q = 0.5$ acidic bicelles, one might speculate that the restriction of motion is mainly due to charge. This is in agreement with structural data obtained by CD where the interaction of penetratin with DHPC micelles and neutral bicelles, as well as with neutral vesicles, induces much less structure than with charged bicelles or vesicles [5,7].

Interestingly, the correlation times for the local motion are similar in all membrane mimetic media (around 1 ns), which shows that the nature of the local motion might be similar in the different mimetics. Similar correlation times for the local motion have been observed previously for the major coat protein from bacteriophage M13 in SDS [38] and for motilin in bicellar solutions [12]. The differences in order parameters, on the other hand, show that the membrane mimetics impose different degrees of restriction on this local motion.

It has previously been argued that the lack of structure in neutral membrane mimetics indicates that penetratin does not interact with neutral membranes. The present study shows that penetratin does interact with neutral bicelles, but probably in a different way as compared with charged bicelles (or micelles). The density of negative charges on the bicelle/micelle surface is seen to affect local dynamics, making penetratin adopt a more rigid structure in charged media than in less charged or neutral media. Finally, it should be pointed out that intrinsic differences between the physical properties of the phospholipid bicelles and phospholipid vesicles could be responsible for the different results concerning peptide–membrane interactions.

Acknowledgements

We thank Drs Jüri Jarvet and Peter Damberg for discussions. This work was supported by the Swedish Research Council.

References

[1] D. Derossi, S. Calvet, A. Trembleau, A. Brunissen, G. Chassaing, A. Prochiantz, Cell internalization of the third helix of the Antennapedia homeodomain is receptor-independent, J. Biol. Chem. 271 (1996) 18188–18193.

[2] J.P. Berlose, O. Convert, D. Derossi, A. Brunissen, G. Chassaing, Conformational and associative behaviours of the third helix of antennapedia homeodomain in membrane–mimetic environments, Eur. J. Biochem. 242 (1996) 372–386.
[3] M. Lindberg, A. Gräslund, The position of the cell penetrating peptide penetratin in SDS micelles determined by NMR, FEBS Lett. 497 (2001) 39–44.
[4] M. Magzoub, L.E.G. Eriksson, A. Gräslund, Conformational states of the cellpenetrating peptide penetratin when interacting with phospholipid vesicles: effects of surface charge and peptide concentration, Biochim. Biophys. Acta 1563 (2002) 53–63.
[5] M. Lindberg, H. Biverståhl, A. Gräslund, L. Mäler, Structure and positioning comparison of two variants of penetratin in two different membrane mimicking systems by NMR, Eur. J. Biochem. 270 (2003) 3055–3063.
[6] M. Magzoub, K. Kilk, L.E.G. Eriksson, U. Langel, A. Gräslund, Interaction and structure induction of cell-penetrating peptides in the presence of phospholipid vesicles, Biochim. Biophys. Acta 1512 (2001) 77–89.
[7] M. Magzoub, L.E.G. Eriksson, A. Gräslund, Comparison of the interaction, positioning, structure induction and membrane perturbation of cell-penetrating peptides and non-translocating variants with phospholipid vesicles, Biophys. Chem. 103 (2001) 271–288.
[8] A. Scheller, B. Wiesner, M. Melzig, M. Bienert, J. Oehlke, Evidence for an amphipathicity independent cellular uptake of amphipathic cell-penetrating peptides, Eur. J. Biochem. 267 (2000) 6043–6050.
[9] R.R. Vold, S.R. Prosser, A.J. Deese, Isotropic solutions of phospholipid bicelles: a new membrane mimetic for high-resolution NMR studies of polypeptides, J. Biomol. NMR 9 (1997) 329–335.
[10] C.R. Sanders, S. Prosser, Bicelles: a model membrane system for all seasons? Structure 6 (1998) 1227–1234.
[11] J.J. Chou, J.D. Kaufman, S.J. Stahl, P.T. Wingfield, A. Bax, Micelle-induced curvature in a water-insoluble HIV-1 Env peptide revealed by NMR dipolar coupling measurement in stretched polyacrylamide gel, J. Am. Chem. Soc. 124 (2002) 2450–2451.
[12] A. Andersson, L. Mäler, NMR solution structure and dynamics of motilin in isotropic phospholipid bicellar solution, J. Biomol. NMR 24 (2002) 103–112.
[13] K.J. Glover, J.A. Whiles, G. Wu, N.-J. Yu, R. Deems, J.O. Struppe, R.E. Stark, E.A. Komives, R.R. Vold, Structural evaluation of phospholipid bicelles for solution-state studies of membrane-associated biomolecules, Biophys. J. 81 (2001) 2163–2171.
[14] P.A. Luchette, T.N. Vetman, R.S. Prosser, R.E.W. Hancock, M.P. Nieh, C.J. Glinka, S. Krueger, J. Katsaras, Morphology of fast-tumbling bicelles: a small angle neutron scattering and NMR study, Biochim. Biophys. Acta 1513 (2001) 83–94.
[15] J.A. Whiles, R. Brasseur, K.J. Glover, G. Melacini, E.A. Komives, R.R. Vold, Orientation and effects of mastoparan X on phospholipid bicelles, Biophys. J. 80 (2001) 280–293.
[16] J. Struppe, J.A. Whiles, R.R. Vold, Acidic phospholipid bicelles: a versatile model membrane system, Biophys. J. 78 (2000) 281–289.
[17] L. Braunschweiler, R.R. Ernst, Coherence transfer by isotropic mixing: applications to proton correlation spectroscopy, J. Magn. Reson. 53 (1983) 535–560.
[18] D.J. States, R.A. Haberkorn, D.J. Ruben, A two-dimensional nuclear Overhauser experiment with pure absorption phase in four quadrants, J. Magn. Reson. 48 (1982) 286–292.
[19] J. Weigelt, Single scan, sensitivity- and gradient-enhanced TROSY for multidimensional experiments, J. Am. Chem. Soc. 120 (1998) 10778–10779.
[20] P.T. Callaghan, M.E. Komlosh, M. Nydén, High magnetic field gradient PGSE NMR in the presence of a large polarizing field, J. Magn. Reson. 133 (1998) 177–182.
[21] E.O. Stejskal, J.E. Tanner, Spin diffusion measurements: spin echoes in the presence of a time dependent field gradient, J. Phys. Chem. 42 (1965) 288–292.
[22] P. Damberg, J. Jarvet, A. Gräslund, Accurate measurement of translational diffusion coefficients: a practical method to account for non-linear gradients, J. Magn. Reson. 148 (2001) 343–348.
[23] N.A. Farrow, R. Muhandiram, A.U. Singer, S.M. Pascal, C.M. Kay, G. Gish, S.E. Shoelson, T. Pawson, J.D. Forman-Kay, L.E. Kay, Backbone dynamics of a free and phosphopeptide-complexed Src homology 2 domain studied by ^{15}N NMR relaxation, Biochemistry 33 (1994) 5984–6003.
[24] B. Lindman, N. Kamenka, M.C. Puyal, R. Rymdén, P. Stilbs, Micelle formation of anionic and cationic surfactants from Fourier transform proton and lithium-7 nuclear magnetic resonance and tracer self-diffusion studies, J. Phys. Chem. 88 (1984) 5048–5057.
[25] A. Andersson, L. Mäler, Motilin–bicelle interactions: membrane position and translational diffusion, FEBS Lett. 545 (2003) 139–143.
[26] G. Lipari, A. Szabo, Model-free approach to the interpretation of nuclear magnetic resonance relaxation in macromolecules: 1. Theory and range of validity, J. Am. Chem. Soc. 104 (1982) 4546–4559.
[27] G. Lipari, A. Szabo, Model-free approach to the interpretation of nuclear magnetic resonance relaxation in macromolecules. 2. Analysis of experimental results, J. Am. Chem. Soc. 104 (1982) 4559–4570.
[28] B. Halle, H. Wennerström, Interpretation of magnetic resonance data from water nuclei in heterogeneous systems, J. Chem. Phys. 75 (1981) 1928–1943.
[29] A.M. Mandel, M. Akke, A.G. Palmer, Backbone dynamics of *Escherichia coli* ribonuclease HI: correlations with structure and function in an active enzyme, J. Mol. Biol. 246 (1995) 144–163.
[30] A.G. Palmer, M. Rance, P. Wright, Intramolecular motions of a zinc finger DNA binding domain from Xfin characterized by proton-detected natural abundance carbon-13 heteronuclear NMR spectroscopy, J. Am. Chem. Soc. 113 (1991) 4371–4380.
[31] P. Damberg, Development of NMR methods for studies of dynamics and structure, Doctoral thesis. Stockholm University, Stockholm, 2001.
[32] M. Ottiger, A. Bax, Determination of relative N–H^N, N–C′, C^α–C′ and C^α–H^α effective bond lengths in a protein by NMR in a dilute liquid crystalline phase, J. Am. Chem. Soc. 120 (1998) 12334–12341.
[33] J. Danielsson, J. Jarvet, P. Damberg, A. Gräslund, Translational diffusion by PFG-NMR on full length and fragments of the Alzheimer Aβ (1–40) peptide. Determination of hydrodynamic radii of random coil peptides of varying length, Magn. Reson. Chem. 40 (2002) S89–S97.
[34] K.J. Glover, J.A. Whiles, R.R. Vold, G. Melacini, Position of residues in transmembrane peptides with respect to the lipid bilayer: a combined lipid NOEs and water chemical exchange approach in phospholipid bicelles, J. Biomol. NMR 22 (2002) 57–64.
[35] J.N. Israelachvili, Intermolecular and Surface Forces, Academic Press, London, 1991.
[36] G.M. Clore, A. Szabo, A. Bax, L.E. Kay, P.C. Driscoll, A.M. Gronenborn, Deviations from the simple two-parameter model-free approach to the interpretation of nitrogen-15 nuclear magnetic relaxation of proteins, J. Am. Chem. Soc. 112 (1990) 4989–4991.
[37] J. Jarvet, J. Zdunek, P. Damberg, A. Gräslund, Three-dimensional structure and position of porcine motilin in sodium dodecyl sulfate micelles determined by ^{1}H NMR, Biochemistry 36 (1997) 8153–8163.
[38] C.H.M. Papavoine, M.L. Remerowski, L.M. Horstink, R.H.N. Konings, C.W. Hilbers, F.J.M. van de Ven, Backbone dynamics of the major coat protein of bacteriophage M13 in detergent micelles by ^{15}N nuclear magnetic resonance relaxation measurements using the model-free approach and reduced spectral density mapping, Biochemistry 36 (1997) 4015–4026.